Germline and somatic genetic variants in the p53 pathway interact to affect cancer risk, progression and drug response

Running title: p53 pathway SNPs and mutations interact to affect cancer

Ping Zhang[1], Isaac Kitchen-Smith[1], Lingyun Xiong[1], Giovanni Stracquadanio[1, 16], Katherine Brown[2, 17], Philipp Richter[1], Marsha Wallace[1], Elisabeth Bond[1], Natasha Sahgal[1], Samantha Moore[1], Svanhild Nornes[1], Sarah De Val[1], Mirvat Surakhy[1], David Sims[2], Xuting Wang[3], Douglas A. Bell[3], Jorge Zeron-Medina[4], Yanyan Jiang[5], Anderson Ryan[5], Joanna Selfe[6], Janet Shipley[6], Siddhartha Kar[7], Paul Pharoah[7], Chey Loveday[8], Rick Jansen[9], Lukasz F. Grochola[10], Claire Palles[11], Andrew Protheroe[13], Val Millar[14], Daniel Ebner[14], Meghana Pagadala[15], Sarah P. Blagden[12], Tim Maughan[12], Enric Domingo[12], Ian Tomlinson[11], Clare Turnbull[8], Hannah Carter[15] and Gareth Bond[1]

[1]Ludwig Institute for Cancer Research, University of Oxford, Nuffield Department of Clinical Medicine, Old Road Campus Research Building, Oxford OX3 7DQ, UK

[2]Weatherall Institute of Molecular Medicine, University of Oxford, John Radcliffe Hospital, Oxford OX3 9DS, UK

[3]Environmental Epigenomics and Disease Group, Immunity, Inflammation, and Disease Laboratory, National Institute of Environmental Health Sciences-National Institutes of Health, Research Triangle Park, NC 27709, USA

[4]Vall d'Hebron University Hospital, Oncology Department, Passeig de la Vall D'Hebron 119, 08035 Barcelona, Spain

[5]CRUK & MRC Oxford Institute for Radiation Oncology, University of Oxford, Department of Oncology, Old Road Campus Research Building, Oxford OX3 7DQ, UK

[6]Sarcoma Molecular Pathology Team, Divisions of Molecular Pathology and Cancer Therapeutics, The Institute of Cancer Research, Sutton, Surrey SM2 5NG, UK.

[7]Department of Public Health and Primary Care, University of Cambridge, Cambridge CB1 8RN, UK

[8]Division of Genetics and Epidemiology, The Institute of Cancer Research, London SW3 6JB, UK

[9]Amsterdam UMC, Vrije Universiteit Amsterdam, Department of Psychiatry, Amsterdam Neuroscience, the Netherlands

[10]Institute for Surgical Pathology, University Hospital of Zurich, Switzerland

[11]Institute of Cancer and Genomic Sciences, University of Birmingham, Birmingham B15 2TT, UK

[12]Department of Oncology, University of Oxford, Oxford OX3 7DQ, UK

[13]Oxford Cancer and Haematology Centre, Oxford University Hospitals NHS Foundation Trust, Oxford OX3 7LE, United Kingdom.

[14]Target Discovery Institute, University of Oxford, Nuffield Department of Medicine, Oxford OX3 7FZ, UK

[15]Department of Medicine, University of California, San Diego, La Jolla, CA 92093, USA

[16] Present address: Institute of Quantitative Biology, Biochemistry, and Biotechnology, SynthSys, School of Biological Sciences, University of Edinburgh, Edinburgh, EH9 3BF, UK

[17] Present address: Division of Virology, Department of Pathology, University of Cambridge, Cambridge, CB2 1QP, UK

Corresponding Authors:

Hannah Carter, UCSD, 9500 Gilman Drive, La Jolla, CA 92093-0688. Phone: 858-822-4706; Fax: 858-822-4246; E-mail: hkcarter@health.ucsd.edu;

Gareth Bond, University of Oxford, Roosevelt Drive, Oxford OX3 7DQ. Phone: 0044-(0)1865-617497; Fax: 0044-(0)1865-617515; E-mail: gareth.bond@ludwig.ox.ac.uk

Declaration of Interests

The authors declare no competing interests.

Abstract

Insights into oncogenesis derived from cancer susceptibility loci (single nucleotide polymorphisms, SNPs) could facilitate better cancer management and treatment through precision oncology. However, therapeutic insights have thus far been limited by our current lack of understanding regarding both interactions of these loci with somatic cancer driver mutations and their influence on tumorigenesis. For example, while both germline and somatic genetic variation to the p53 tumor suppressor pathway are known to promote tumorigenesis, little is known about the extent to which such variants cooperate to alter pathway activity. Here we hypothesize that cancer risk-associated germline variants interact with somatic p53 mutational status to modify cancer risk, progression and response to therapy. First, we provide supportive evidence for this hypothesis by focusing on a cancer risk SNP (rs78378222) with a well-documented ability to directly influence p53 activity, and by integrating germline datasets relating to cancer susceptibility with tumor data capturing somatically-acquired genetic variation. We go on to demonstrate that through the integration of germline and somatic genetic data, we can identify a novel entry point for therapeutically manipulating p53 activities. We provide evidence that a cluster of cancer risk SNPs result in increased expression of a pro-survival p53 target gene (KITLG) and attenuation of p53-mediated responses to genotoxic therapies, which can be reversed by pharmacological inhibition of the pro-survival cKIT signal. Together, our results offer evidence of how cancer susceptibility SNPs can interact with cancer driver genes to affect cancer progression and identify novel combinatorial therapies.

Significance

We describe significant interactions between heritable and somatic genetic variants in the p53 pathway that affect cancer susceptibility, progression and treatment response. Our results offer evidence of how cancer susceptibility SNPs can interact with cancer driver genes to affect cancer progression and identify novel therapeutic targets.

Introduction

Efforts to characterize the somatic alterations that drive oncogenesis have led to the development of targeted therapies, facilitating precision approaches that condition treatment on knowledge of the tumor genome, and improving outcomes for many cancer patients (1,2). However, such targeted therapies are associated with variable responses, eventual high failure rates and the development of drug resistance. Somatic genetic heterogeneity among tumors is a major factor contributing to differences in disease progression and therapeutic response (1). Interindividual differences may arise not only from different somatic alterations, but also from differences in the underlying genetic background. The maps of common germline genetic variants that associate with disease susceptibility allow us to generate and test biological hypotheses, characterize regulatory mechanisms by which variants contribute to disease, with the aim of integrating the results into the clinic. However, there are challenges in harnessing of susceptibility loci for target identification for cancer, including limitations in (i) exposition of causative variants within susceptibility loci, (ii) understanding of interactions of susceptibility variants with somatic driver mutations, and (iii) mechanistic insights into their influence on cellular behaviors during and after the evolution of somatic cancer genomes (3-5).

A key cancer signaling pathway known to harbor multiple germline and somatic variants associated with cancer susceptibility is the p53 tumor suppressor pathway (6). It is a stress response pathway that maintains genomic integrity and is among the most commonly perturbed pathways in cancer, with somatic driver mutations found in the *TP53* gene in more than 50% of cancer genomes (7). Loss of the pathway and/or the gain of pro-cancer mutations can lead to cellular transformation and tumorigenesis (8). Once cancer has developed, the p53 pathway is important in mediating cancer progression and the response to therapy, as its anti-cancer activities can be activated by many genotoxic anticancer drugs (9). These drugs are more effective in killing cancers with wild-type p53 relative to mutant p53 (10,11). While both germline and somatic alterations to the p53 pathway are known to promote tumorigenesis, the extent to which such variants cooperate to alter pathway activity and the effects on response to therapy remain poorly understood.

Most studies have separately examined the consequences of somatic and germline variation affecting p53 activity to understand their roles in disease risk, progression or response to therapy. Here we hypothesize that cancer-associated germline variants (single nucleotide polymorphisms, SNPs) interact with p53 somatic driver mutations to modify cancer risk, progression and potential to respond to therapy. With a focus on a cancer-associated SNP that directly influences p53 activity, we

provide supportive evidence for this hypothesis, and go on to demonstrate how such germline-somatic interactions inform discovery of candidate drug targets.

Materials and Methods

Assigning p53 mutational status to breast, ovarian cancers and TCGA tumors

We curated *TP53* pathogenic missense mutations by integrating up-to-date functional evidence from both literature and databases as detailed in Supplementary Information. In total, we were able to find 218 out of 323 TP53 pathogenic mutations are oncogenic (**Supplementary Table S7**). All TP53 missense mutations in breast, ovarian cancers and TCGA primary tumors were extracted and matched with the curated lists of pathogenic and oncogenic TP53 missense mutations..

Analysis for subtype heterogeneity SNPs with Breast and Ovarian cancer association studies

Estimates of effect sizes [log(OR)s] for subtype-specific case-control studies and their corresponding standard errors were utilized for meta- and heterogeneity-analyses using METAL (2011-03-25 release) (12), under an inverse variance fixed-effect model. See Supplementary Information for details.

Cancer GWAS SNPs

We selected the GWAS significant lead SNPs (p-value <5e-08) in Europeans, and retrieved the associated proxy SNPs using the 1000 Genomes phase 3 data through the web server rAggr. See Supplementary Information for details.

Enrichment analysis

The hypergeometric distribution enrichment analysis was performed as described in (6). Significance was determined using PHYPER function as implemented in R and multiple hypotheses testing by Benjamini-Hochberg correction.

Genotype imputation and population stratification

Genotype data was obtained and filtered as described in (3). The genotype data of 7,021 TCGA patients were clustered tightly with Europeans. See Supplementary Information for details.

TCGA survival analysis

The omics datasets (gene mutation, copy number and mRNA expression) of the TCGA cohort were downloaded from the cBioPortal (https://www.cbioportal.org/). We considered those mutations with putative oncogenic properties (marked as 'Oncogenic', 'Likely Oncogenic' or 'Predicted Oncogenic' in OncoKB) as oncogenic mutations. TCGA clinical data was downloaded from recently updated Pan-Cancer Clinical Data Resource (TCGA-CDR) (13). TCGA clinical radiation data was retrieved using R package TCGAbiolinks (V2.16.1). The patients with "Radiographic Progressive Disease" were defined as radiation non-responders, and with "Complete Response" or "Partial Response" were defined as responders. A Cox proportional hazards regression model was used to calculate the hazard ratio, the 95% confidence interval and p values for two-group comparisons. The log-rank test was used to compare the difference of Kaplan-Meier survival curves. The clinical, gene expression and mutation data for the DFCI-SKCM cohort was downloaded from cBioPortal. The optimal cut-off of the gene expression for the survival analysis was determined using the survcutpoint function of the survminer R package, and used to stratify the patients into high- and low-risk groups.

GDSC drug sensitivity analysis

TP53 mutation, copy number, RNAseq gene expression data, and drug IC50 values for the cancer cell lines were downloaded from Genomics of Drug Sensitivity in Cancer (GDSC; release-8.1). The classified cell lines based on p53 mutational status were further grouped based on the gene transcript levels: low (≤ 1st quartile), intermediate (> 1st quartile and < 3rd quartile), high (≥ 3rd quartile). The effects of the mutation status or transcript levels on drug sensitivity were then determined with a linear model approach. See details in Supplementary Information.

Cell culture and their treatments

Testicular cancer cell lines TERA1, TERA2, 2102EP, Susa-CR, GH, were cultured in RPMI medium containing 10% fetal bovine serum and 1% penicillin/streptomycin according to standard conditions. Susa cells were cultured in RPMI medium containing 20% fetal bovine and 1% penicillin/streptomycin. GCT27 and GCT27-CR were cultured in DMEM supplemented with 10%

fetal bovine serum and 1% penicillin/streptomycin. Hap1 cells were obtained from Horizon Discovery Ltd and cultured in IMDM (Sigma-Aldrich Co Ltd) supplemented with 10% fetal bovine serum and 1% penicillin/streptomycin. FuGENE 6 Transfection Reagent (Promega) was used for DNA transfection. For transfection of siRNA, Lipofectamine RNAiMAX Transfection Reagent (ThermoFisher) was used. The cell lines were tested as Mycoplasma contamination negative every 3-4 weeks using MycoAlert™ mycoplasma detection kit (Lonza), and used for experiments at less than 20 passages. Cell line authentication was performed by STR (Short Tandem Repeat) analysis (Eurofins Genomics).

CRISPR/Cas9-mediated genome editing

The Cas9 expression vector was obtained from Addgene (#62988). sgRNAs were designed and constructed as described previously (14). The oligo sequences for the sgRNA synthesis are listed in **Supplementary Table S8**. See Supplementary Information for details.

RNA isolation, qRT-PCR and RNA-seq analysis

RNA isolation, qRT-PCR and RNA-seq analysis were performed as detailed in Supplementary Information.

Drug screening

Cells were seeded in 384-well plates (flat bottom, black with clear bottom, Greiner) at density of about 2,000 cells per well in 81µl with cell dispenser (PerkinElmer) and liquid handling robotics (JANUS, PerkinElmer) and incubated overnight. Next, library compounds (**Supplementary Table S5**) were added to a final concentration of 10µM, 1µM, 100nM or 10nM. Dasatinib (1uM) was added as positive control and DMSO (Vehicle, 0.1%) was added as negative control. After 72 hours, cell were fixed with 4% paraformaldehyde for 10 min, permeabilized with 0.5% Triton X-100 for 5 min, and then stained with 1:1000 dilution of 5mg/ml DAPI for 5 min. Next, the plates were imaged using a high-content analysis system (Operetta, PerkinElmer). The image data was analyzed by an image data storage and analysis system (Columbus, PerkinElmer). The cells with nuclear area>150 and nuclear intensity<700 were counted, and cell number was used as the viability readout. The screen was performed in duplicate. The Pearson Correlation Coefficient, a measurement for inter-assay variability, averaged 0.98 and an average Z-factor, a measure employed in high throughput

screens to measure effect size, of 0.69 for all plates was recorded, leading to high confidence in the primary screen positive hits (**Supplementary Table S6**).

SDS-PAGE and western blotting

SDS-PAGE and western blotting was performed as described in (15). The antibodies against p53 (sc-126), c-KIT (sc-17806), PARP1 (sc-7150), and β-Actin (sc-47778) were from Santa Cruz (Dallas, TX, USA). The antibodies against acetylated p53 (Lys382, #2525), cleaved Caspase 3 (Asp175, #9661) were from Cell Signaling. HRP-coupled secondary antibodies were from Dako.

IC50 and combination index CI analyses

To determine an IC50, 8 multiply diluted concentrations were used including a PBS control for 48 hour treatment and then cell viability was assessed by a MTT assay (see details in Supplementary Information). The IC50 was calculated using the Graphpad Prism software. A constant ratio matrix approach was used to determine the combination index CI values (16). Single drug data and combination data was entered into Compusyn software (http://www.combosyn.com) to compute CI50 and dose-reduction index (DRI). CI50 is (CX/IC50(X)) + (CY/IC50(Y)), where (CX/IC50(X)) is the ratio of the drug X's concentration (CX) in a 50% effective drug mixture to its 50% inhibitory concentration (IC50(X)) when applied alone. The CI50 values quantitatively depict synergistic (CI<1), additive (CI=1), and antagonistic effects (CI>1).

In vivo study

All animal procedures were carried out under a Home Office licence (PPL30/3395), and mice were housed at Oxford University Biomedical Services, UK. 6-8 week-old female BALB/c nude mice (Charles River, UK) were injected subcutaneously. See Supplementary Information for details.

Results

1. p53 regulatory cancer risk SNP rs78378222 associates with subtype heterogeneity

To represent germline effects, we focused on the cancer-associated SNP with the most direct and most understood influence on p53 activity. This SNP, rs78378222, resides in the 3'-UTR in the canonical *TP53* polyadenylation signal (p53 poly(A) SNP). The minor C-allele is known to associate

with lower p53 mRNA levels in different normal tissue types, such as in blood, skin, adipose, esophagus-mucosa, and fibroblasts (17,18), and associate strongly with differential risk of many cancer types (19-23).

We explored whether the p53 poly(A) SNP can differentially influence mutant and wtp53 cancer risk by studying cancers with subtypes that differ substantially in p53 mutation frequencies and for which susceptibility GWAS data are available. 18% of estrogen receptor positive breast cancers (ER+BC) mutate p53, in contrast to 76% of estrogen receptor negative breast cancers (ER-BC) (24). Similarly, less than 10% of low-grade serous ovarian cancers (LGSOC) mutate p53, in contrast to 96% of high grade serous ovarian cancers (HGSOC) (25). Over 85% of p53 pathogenic missense mutations in breast and ovarian cancers are oncogenic (either dominant negative or gain-of-function) (**Fig. 1A**) (see Methods). We analyzed data from 90,969 breast cancer patients of European ancestry (69,501 ER-pos BC, 21,468 ER-neg BC) (26) and 105,974 controls, and 14,049 ovarian cancer patients of European ancestry (1,012 LGSOC, 13,037 HGSOC) and 40,941 controls (27).

It is known that key regulatory pathway genes and stress signals, which can regulate wild-type p53 (wtp53) levels and tumor suppressive activities, can also regulate mutant p53, including its oncogenic activities (28,29). Thus, if the poly(A) SNP can influence both mutant and wtp53, the minor C-allele (less p53 expression) would be expected to have opposite associations with disease subtype (**Fig. 1B**). That is, the minor C-allele would associate with increased cancer risk (OR>1) in the subtypes with low p53 mutation frequencies (ER+BC and LGSOC), and decreased cancer risk (OR<1) in the subtypes with high p53 mutation frequencies (ER-BC and HGSOC). Indeed, this is the case, whereby we found an increase in the frequency of the minor C-allele in ER+BC and LGSOC patients compared to healthy controls (OR=1.12, p=9.98e-04 and OR=1.59, p=0.016, respectively) (**Fig. 1C**), but a decreased frequency in ER-BC and HGSOC patients compared to controls (OR=0.80, p=2.30e-04 and OR=0.75, p=3.68e-04, respectively). Taken together, the distribution of minor C-allele shows significant heterogeneity among the four cancer subtypes (p-het=2.59e-09).

The above analysis supports a persistent effect for the p53 cancer risk SNP on tumors through a possible influence on whether or not a tumor contains a somatically mutated *TP53* locus. In order to seek further and more direct support of this possibility, we performed similar analyses of the p53 poly(A) SNP in a cohort of 7,021 patients of European origin diagnosed with 31 different cancers and for whom the p53 mutational status of their cancers could be determined (The Cancer Genome Atlas, TCGA). We partitioned the patients into two groups based on the presence or absence of the p53 somatic alteration (mutation and CNV loss versus WT and no CNV loss; (**Fig. 1D**).

Interestingly, the TP53 poly(A) SNP associated with allelic differences in minor allele frequencies between the groups of patients with either p53 WT or mutant tumors (**Fig. 1E**). This is in line with the associations found with p53 mutational status, whereby the C-allele is more frequent in wtp53 tumors.

2. A p53 regulatory cancer risk SNP can affect wild type and mutant p53 in tumors, and associates with clinical outcomes.

As mentioned above, the minor C-allele of the TP53 poly(A) SNP has been previously found to associate with lower p53 mRNA levels in many different normal tissues and cells (18). To investigate the activity of this SNP in tumors, we analyzed expression data from 3,248 tumors from the TCGA cohort, for which both germline and somatic genetic data are available and no somatic copy number variation of p53 could be detected. Similar to results obtained in the normal tissues, we observed a significant association of the minor C-allele with lower p53 expression levels in the tumors, estimated 1.5-fold per allele (p=1.7e-04, beta=-0.37; **Fig. 2A**). To test if the C-allele associates with lower levels of both wild type and mutant p53, we divided the tumors into three groups based on their respective somatic p53 mutational status (**Supplementary Fig. 1A** and **Supplementary Table S1**). We found 2,521 tumors with wtp53, 448 with missense mutations, and, of those, 389 with oncogenic missense mutations. In all three groups, the C-allele significantly associates with lower p53 expression levels (**Supplementary Fig. 1B**).

Next, we utilized Hap1 cells that contain a dominant-negative p53 missense mutation (p.S215G), which results in a mutated DNA-binding domain (30). We generated clones with either the A-allele or the C-allele (**Fig. 2B**), and found significantly lower p53 mRNA levels in cells with the C-allele relative to the A-allele (~2 fold, **Fig. 2C**). We also found the C-allele containing cells express less p53 protein (**Supplementary Fig. 1C**). The impairment of 3'-end processing and subsequent transcription termination by the minor allele of the p53 poly(A) SNP, have been proposed as a mechanism for the genotype-dependent regulatory effects on p53 expression (17). Indeed, we observed significant enrichments of uncleaved p53 mRNA in cells carrying the C-allele compared to the A-allele by qRT-PCR and 3' RNA-sequencing (**Supplementary Fig. 1D-E**). Together, our data demonstrate that this cancer risk-associated SNP can influence the expression of both wild type and mutant p53 in cancer cells and tumors.

To explore whether the p53 poly(A) SNP also associates with allelic differences in clinical outcomes, we stratified the TCGA cohort into two groups based on p53 somatic alterations and the p53 poly(A) SNP genotypes. We found that in patients with wtp53 tumors, those with the minor C-

alleles have a significantly shorter PFI and worse OS compared to those without the minor alleles (**Fig. 2D**), but not in patients without stratification. An inverted, but not significant trend, among the patients with somatic *TP53* mutations is noted. Similarly, significant, p53 mutational status-dependent, associations between the p53 poly(A) SNP and PFI can be found when we restrict our analyses to breast cancer patients only (**Fig. 2E**).

It is well documented that p53 somatic mutations antagonise cellular sensitivity to radiotherapy (31), an important component of current cancer treatments. Indeed, we see not only TP53 mutations, but also the p53 poly(A) SNP play roles in radiation response phenotype in the TCGA cohort. Specifically, we focused on the 7021 patients for whom the SNP genotypes were available. Of these, 848 patients could be assigned with radiation response phenotypes (603 responders; 134 non-responders; see Methods). We determined that the radiation non-responders were significantly enriched in patients with TP53 somatic mutations (OR= 1.6, p = 0.021; **Fig. 2F**). The enrichment was further enhanced when we analysed those patients with both TP53 mutations and copy number loss (OR = 2.2, p = 0.0026). Importantly, we also found that in patients with wtp53 tumors, but not with p53 mutant tumors, radiation non-responders were greatly enriched in the C-allele of the p53 poly(A) SNP (less p53 expression (OR = 5.6, p = 0.011 for risk allele; **Fig. 2F**).

3. Somatic copy number loss of p53 can mimic effects of the p53 poly(A) SNP

Together, the results we have presented thus-far suggest that the relative 2-fold reduction of wtp53 levels in tumors from patients with the minor allele of the p53 regulatory SNP can lead to worse clinical outcomes and treatment response. If true, we reasoned that we should be able to find similar associations in patients whose tumors lose a single copy of p53. In the TGCA database, 1839 (26.6%) patients with wtp53 tumors, and 2236 (59.3%) patients with mutant p53 tumors show significant signs of loss at the p53 locus (estimated one copy on average, GISTIC score -1). These tumors associate with 1.3-fold and 1.1-fold lower p53 RNA expression respectively compared to the tumors without loss (**Fig. 2G**). In support of small reductions of p53 expression affecting patient outcome, we found that wtp53-loss associates with shorter PFI and worse OS compared to no p53-losses (**Fig. 2H**), but are not found in patients with mutant p53. These associations are independent of tumor type (adjusted $p < 0.05$; **Fig. 2H**). We also found in patients with p53 WT tumors, that radiotherapy non-responders are significantly enriched in cancers with p53 copy number loss (OR =1.6, p = 0.027; **Fig. 2I**).

We next sought to test whether the modest changes in p53 expression (<2 fold) could predict chemosensitivities. We used the drug sensitivity dataset with both somatic genetic and gene

expression data (GDSC; 304 drugs across 987 cell lines). Similar to what we observed in TCGA tumors, p53 copy number loss in cancer cell lines associates with a modest reduction in p53 expression (**Fig. 3A**). Strikingly, and as predicted, wtp53 loss, but not mutant p53-loss, significantly associates with reduced sensitivities to 31% of the drugs tested (**Fig. 3B; Supplementary Table S2**). Specifically, 93 out of the 304 drugs demonstrated reduced sensitivity in wtp53 cell lines with TP53-loss compared to those without a loss (adjusted $p < 0.05$; **Fig. 3B**). These drugs included many known p53 activating agents including an MDM2 inhibitor (Nutlin3), as well as standard chemotherapeutics such as cisplatin, doxorubicin, and etoposide. Together, our observations clearly indicate that patients whose tumors have modest decreases in wtp53 expression, mediated either through the regulatory SNP or somatic p53 copy number loss, associate with poorer DNA-damage responses and clinical outcomes.

4. A drug-able p53 pathway gene with cancer risk SNPs associates with pathway inhibitory traits

Various therapeutic efforts have been designed around restoring wtp53 activity to improve p53-mediated cell killing (32). The identification of a p53 regulatory cancer risk SNP that affects, in tumors, p53 expression levels, activity, p53 mutational status, tumor progression, outcome and radiation responses (as demonstrated for the p53 poly(A) SNP) points to other potential entry points for therapeutically manipulating p53 activities guided by these commonly inherited cancer risk variants. We reasoned that p53 pathway genes with alleles which increase expression of genes that inhibit p53 cell-killing activities and increase cancer risk, would be potential drug targets to re-activate p53 through their inhibition.

In total, there are 1,133 GWAS implicated cancer-risk SNPs (lead SNPs and proxies) in 41 out of 410 annotated p53 pathway genes (KEGG, BioCarta and PANTHER and/or direct p53 target genes (33)) (**Fig. 3C; Supplementary Table S3**). To systematically identify those p53 pathway genes with cancer risk SNPs whose increased expression associates with inhibition of p53-mediated cancer cell killing, we looked to the above-described drug sensitivity dataset with both somatic genetic and gene expression data (34). In total, the transcript levels of 3 of the 41 p53 pathway genes that harbor cancer risk SNPs associate with Nutlin3 (the most significant compound associated with wtp53 CNV status) sensitivities in cell lines with WT *TP53* and no copy number loss compared to those with *TP53* mutations (KITLG, CDKN2A and TEX9; adjusted $p < 0.05$; **Fig. 3D**). For all three of the significant associations, increased expression of these genes associates with increased resistance to Nutlin3 treatment. In order to further validate these associations in terms of their dependency on p53 activation and not solely Nutlin3 treatment, we explored similar associations in

the other three DNA-damaging agents (Doxorubicin, Etoposide and Cisplatin) that demonstrated sensitivities to p53 mutational status (**Fig. 3B**). Only for KITLG (**Fig. 3E**), did increased expression levels associate with increased resistance towards all four agents.

5. Increased expression of KITLG attenuates p53's anti-cancer activities

There are multiple significant associations that are consistent with an inhibitory role of increased KITLG expression on p53's anti-cancer activities in TGCT, a cancer type that rarely mutates p53. First, relative to other cancer types, KITLG copy gain (GISTIC score ≥1) is highly enriched in wtp53 tumors of (3.7-fold, adjusted p = 2.9e-29; **Fig. 4A**). Second, the TGCT GWAS risk allele residing in KITLG is enriched in TGCT patients with wtp53 tumors relative to the wtp53 tumors of other cancer types (**Fig. 4B**). Third, patients with elevated expression of KITLG in wtp53 TGCT progress faster (**Fig. 4C**). Fourth, the TGCT GWAS risk locus falls within an intron of *KITLG* occupied by p53 in many different cell types and under many different cellular stresses (**Supplementary Fig. 2A**). This region contains 6 common SNP that are in high linkage disequilibrium (LD) in Europeans (r^2 >0.95) (red square, **Fig. 4D**) (35,36), including a reported polymorphic p53 response element (p53 RE SNP, rs4590952). The major alleles of this SNP associate with increased TGCT risk, increased p53 binding, transcriptional enhancer activity, and greater KITLG expression in heterozygous cancer cell lines wild type for p53 (37). Third, higher grade, but not lower grade, wtp53 TGCT patients carrying alleles associated with increased risk and KITLG expression also progress faster (**Fig. 4E and Supplementary Fig. 2B-C; Supplementary Table S4**).

In order to experimentally test the potential inhibitory role of increased KITLG expression on p53's anti-cancer activities in TGCT, we deleted the risk locus in two TGCT-derived cell lines (TERA1 and TERA2) with wtp53 and homozygous for the TGCT risk alleles (p53-REs+/+) (**Fig. 4F and Supplementary Fig. S3A-C**). As predicted from the above-described associations, we found significantly higher *KITLG* RNA levels in non-edited p53-REs+/+ clones, compared to either the heterozygous KOs p53-REs+/- clones or the homozygous KOs REs-/- clones (**Fig. 4G**). After Nutlin3 treatment, the p53-REs-/- clones showed no measurable induction of *KITLG* relative to p53-RE+/+ cells (**Fig. 4H**, red bars versus grey bars). We found no significant differences between the p53-REs-/- and p53-REs+/+ clones in other genes surrounding KITLG (±1Mbp; **Supplementary Fig.** S3D). Re-integration of the deleted regions into its original locus rescued basal expression, resulting in significantly higher *KITLG* RNA levels in the knock-in (KI) clones of both cell lines relative to the p53-REs-/- (**Fig. 4F and 4I; Supplementary Fig. S3E-G**). The KI clones also rescued the p53-dependent induction of *KITLG* expression relative to the p53-REs-/- (**Fig. 4I**).

KITLG is best known to act through the c-KIT receptor tyrosine kinase to promote cell survival in many cancer types (38). To determine if heightened *KITLG*/c-KIT signaling inhibits p53's anti-cancer activities in TGCT, we explored its impact on cellular sensitivities to p53-activating agents. We found that deletion of the KITLG risk locus or c-KIT knock-down resulted in an increased sensitivity to Nultlin3, and increased levels of cleaved caspase3 and PARP1 (**Fig. 5A-B; Supplementary Fig. S4A-B**). We were able to rescue the increased Nutlin3 sensitivity and caspase3/PARP1 cleavage of p53RE-/- clones in KI cells (**Fig. 5A and Supplementary Fig.S4C**). To further test the p53-dependence of these effects, we reduced p53 expression levels and observed reduced expression of cleaved caspase3 after Nutlin3 treatment (**Supplementary Fig. S4D**), and an overall insensitivity towards Nutlin3 in both p53-REs+/+ and p53-REs-/- cells (**Supplementary Fig. S4E).**

Thus-far, we have demonstrated that TGCT cells with increased expression of *KITLG* have increased pro-cancer survival traits previously attributed to KITLG/cKIT signaling in other cancer types. Moreover, these cells also have traits that suggest an inhibitory effect of KITLG on a p53-associated anti-cancer activity, namely the apoptotic response to p53 activation after MDM2 inhibition with Nutlin3 treatment. To further explore this, we screened 317 anti-cancer compounds to identify agents that, like Nutlin3, kill significantly more cells at lower concentrations in p53-RE-/- clones than in p53+/+ clones (**Fig. 5C**). We identified 198 compounds in the TERA1 screen and 112 compounds in the TERA2 screen that showed heightened sensitivity in p53-RE-/- cells in at least one of the 4 different concentrations tested (≥1.5 fold in both replicates; **Supplementary Fig. S5A**, blue dots). One hundred of these agents overlapped between TERA1 and TERA2 (1.7-fold, p = 1.1e-21; **Supplementary Fig. S5A**), suggesting a potential shared mechanism underling the differential sensitivities. For example, two *MDM2* inhibitors in the panel of compounds, Nutlin3 and Serdemetan, were among the 100 overlapping agents (**Fig. 5D; Supplementary Table S5**). We found a significant and consistent enrichment of topoisomerase inhibitors in both cell lines among 14 different compound classes (14 compounds in TERA1 [100%] and 10 compounds in TERA2 [71%] of 14 Topo inhibitors screened; **Fig. 5D-E**). To validate the genotype-specific effects of the topoisomerase inhibitors, we determined the IC50 values of three of them, Doxorubicin, Camptothecin. and Topotecan, using MTT measurements in multiple clones of TERA1 cells with differing genotypes. All three agents showed a significant reduction of IC50 values, increased sensitivities, in the p53-REs-/- clones (lower KITLG) relative to the p53-REs+/+ clones (higher KITLG) (**Supplementary Fig. S5B**). We were able to rescue this increased sensitivity to topoisomerase inhibitors in the p53RE-/- clones in KI cells (**Supplementary Fig. S5B**). Together,

these results demonstrate that TGCT cell lines with heightened KITLG expression mediated by the risk locus, are less sensitive to 100 agents most of which are known to activate p53-mediated cell killing.

6. Inhibition of KITLG/c-KIT signaling and p53 activation interact to kill treatment resistant cancer cells

There are many RTK inhibitors that are current therapeutic agents which inhibit c-KIT activity (39). If p53-mediated *KITLG*-dependent pro-survival signaling can attenuate chemosensitivity to p53-activating agents, RTK inhibitors should be able to interact synergistically with p53-activating agents to kill TGCT cells. Indeed, co-modulation of these two pathways has shown promise in other cancer types (40-42). We therefore tested which RTK inhibitor (known to inhibit c-KIT) kills TCGT cells most efficiently. Of the five FDA-approved RTKs analyzed, Pazopanib, Imatinib, Nilotinib, Suntinib and Dasatinib, the most potent was Dasatinib (**Supplementary Fig. S5C**). To determine potential synergy of RTKs with Nutlin3 in TGCT, we treated cells with Dasatinib, and quantitated potential drug-drug interactions by calculating Combination Indices (CI). We observed clear synergistic interactions (CI <1) between Nutlin3 and Dasatinib in both TERA1 and TERA2 p53-REs+/+ cells (**Fig. 5F**, grey bars), and enhanced levels of cleaved caspase3 and PARP1, relative to single drug treatments without altering p53 stabilization (**Supplementary Fig. S5D**). Consistent with the requirement of the p53-dependent activation of *KITLG*, no synergy between Dasatanib and Nutlin3 was detected in p53-REs-/- cells (CI>1; **Fig. 5F**, red bars).

We next explored the interaction between Dasatinib and multiple DNA-damaging chemotherapeutics known to activate p53. We focused on the 3 topoisomerase inhibitors (Doxorubicin, Camptothecin and Topotecan), as well as Cisplatin, a chemotherapeutic agent used to treat TGCT, and which induces DNA damage and p53. Dasatinib demonstrated significant levels of synergy with each of the DNA-damaging agents tested in p53-REs+/+ cells (**Supplementary Fig. S5E-F**). Similar to Nutlin3, no synergy was detected in p53-REs-/- cells of either cell lines for any combination of agents (**Supplementary Fig. S5E-F**). Furthermore, the synergistic interaction between Dasatinib and the p53-activating agents Nutlin3 and Doxorubin could be rescued by knocking in the p53-bound germline TGCT-risk locus in *KITLG* (**Fig. 5G**, orange bars).

Thus, a more effective therapeutic strategy for TGCT patients could be to modulate both the cell death and cell survival functions of p53, through co-inhibition of p53/*KITLG*-mediated pro-survival signaling together with the co-activation of p53-mediated anti-survival signaling. Such a therapeutic combination could provide an alternative for patients with treatment-resistant disease (43). To

investigate this idea, we explored synergistic interactions between c-KIT inhibitor Dasatinib and p53 activators in cisplatin-resistant clones of GCT27 (GCT27-CR) and Susa (Susa-CR) (44), as well as in the intrinsically cisplatin-resistant TGCT cell line 2102EP (45) with wtp53 and at least one copy of the haplotype containing the KITLG risk allele SNPs. Similar to the observations in the cisplatin-sensitive TGCT cell lines, Dasatinib and Doxorubicin interacted synergistically to kill all three cisplatin-resistant clones and cell lines (**Fig. 5H**). Moreover, co-treatment with Dasatinib and Doxorubicin of Susa-CR and 2102EP led to a significant reduction (~20-fold on average) in the concentrations of Dasatinib and Doxorubicin used to achieve IC50 relative to when the drugs are used individually (**Supplementary Fig. S5G**). To determine if the combination treatment could show a greater efficacy in treating tumors, we generated a subcutaneous xenograft model using the 2102EP cell line, and treated the mice with two approved drugs Dasatinib and Doxorubicin either alone or in combination. Consistent with the observations made in cell culture, treatment of mice engrafted with 2102EP cells revealed stronger anti-tumoral effects with the Dasatinib/Doxorubicin pair relative to single drug treatments (**Fig. 5I**). This dosing regimen was well tolerated with no body weight loss in mice (**Supplementary Fig. S5H**).

7. KITLG/c-KIT signaling interacts with p53 to affect cancer progression and drug response in melanoma

Our results clearly support a model, whereby increased expression of KITLG mediated by the region with the TGCT cancer risk SNP(s) heightens KITLG/c-KIT signaling and attenuates p53 activity, thereby allowing for the retention and re-activation of wtp53 in testicular cancer cells. The KITLG testicular cancer risk SNP(s) have yet to be found to associate with other cancer types (46), suggesting a tissue-specificity of this locus with enhancer activity. However, other genetic variants that elevate KITLG/c-KIT signaling could also attenuate p53 activity, and thus allow for the retention and ultimate re-activation of wtp53 in cancer cells. To test this, we focused on known somatic driver mutations of c-KIT in the TCGA cohort. If our model is correct, we would expect the majority of tumors with activating c-KIT mutations to retain a wtp53 locus. Indeed, 43 out of 6,997 (0.61%) patients with wtp53 tumors also have oncogenic c-KIT mutations relative to just 10 out of 3,735 (0.27%) of TP53 mutant tumors (**Fig. 6A**; OR = 2.3, p = 0.014).

As expected, the tumor types enriched in c-KIT oncogenic mutations in the TCGA cohort are cancers known to be driven by KIT signaling (38). Testicular cancers (TGCT; 13.6%; 20 out of 147), skin cutaneous melanoma (SKCM; 3.9%; 14 out of 356) and acute myeloid leukemias (AML; 2.8%; 5 out of 181) have proportionally more cKIT mutations than all wtp53 tumors (0.61%) (adjusted p <0.05; **Fig. 6B** left panel). It is important to note that these enrichments are only

significant when wtp53 without TP53-loss, but not p53 loss or mutant tumors are considered (**Fig. 6B**). If our model is correct and inhibition of c-KIT signaling will re-activate p53's ability to kill the wtp53 cancers, we would expect, like in TGCT, that elevated KITLG levels will associate with faster progression and/or poorer survival of the cancers with both wild-type p53 and c-KIT. Indeed, in both melanoma and AML, we observed the association between heightened KITLG expression and poorer clinical outcomes (**Fig. 6C**, the TCGA-SKCM cohort; **Fig. 6D** the TCGA-AML cohort). Consistent associations were observed in an independent cohort (DFCI-SKCM) of 35 wtp53 melanoma patients (**Fig. 6E),** for which both the somatic genetic and expression data are available (47). Importantly, we found that in melanoma and AML patients with wtp53 and no copy number loss tumors, those with heightened KITLG expression have a significantly poorer outcomes, but not in patients with *TP53* mutant or copy number loss (**Fig. 6F-G**). Together these observations, suggest that heightened KITLG/cKIT signaling in AML and melanoma could attenuate p53 activity allowing for wtp53 retention and re-activation using cKIT inh ibitors. In further support of this, in AML, it has been shown that the c-Kit inhibitor dasatinib does enhance p53-mediated cell killing (40). Similarly, when we treated melanoma cells (SKMEL5 with wtp53 and wild type c-KIT) with Dasatinib and the p53 activating agents Nutlin3 or Doxorubicin, we observed clear synergistic interactions (**Fig. 6H**, CI <1; p = 0.0013 between Nutlin3 and Dasatinib and p= 0.00066 between Doxorubicin and Dasatinib).

Discussion

In this study, we demonstrate that germline cancer-risk SNPs could influence cancer progression and potentially provide information guiding precision medicine therapy decisions. Our work highlights that even small relative reductions in wtp53 expression, mediated either by the minor allele of the p53 poly(A) SNP or through loss of at least one copy of TP53, can reduce relative p53 cellular activity in cancer cells and overall survival of patients. Patients with either of these genetic variations represent a large proportion of cancer patients. Patients with the minor allele of the SNP and wtp53 in their cancers are found in 2.6% of the total TCGA cohort, with up to 5.9% in 27 different cancers. Overall, in the TCGA, 26.6% patients have cancers wherein at least one copy loss of wtp53 with up to 73.1% in 32 different cancers. In terms of including p53 status in prognosis for patients, p53 mutation is often what is looked at most. Our work suggests that wtp53 loss could also add additional information to those patients that retain wtp53. Indeed, patients with tumors that express lower wtp53 levels will be interesting to study more in depth to understand how to increase

wtp53 expression to improve treatments, such as increasing transcription of wtp53, inhibiting miRNAs or blocking alternative polyadenylation.

The p53 stress response pathway inhibits cell survival, mediating both tumor suppression and cellular responses to many cancer therapeutics (48). p53 also targets pro-survival genes. Activation of these genes in tumors retaining wild-type p53 provide a survival advantage (49). We provide human genetic evidence that also supports a tumor-promoting role of p53 pro-survival activities and, in the case of the TGCT risk locus, points to the development of more effective therapy combinations through the inhibition of these pro-survival activities in tumors that retain p53 activity. Although TGCTs are one of the most curable solid tumors, men diagnosed with metastatic TGCT develop platinum resistant disease and die at an average age of 32 years (43). There have been few new treatments developed in the last two decades, and current therapeutic approaches can, importantly in context of a cancer of young men, result in significant survivorship issues, including sustained morbidities and delayed major sequelae (43). Our observations suggest the TGCT *KITLG* risk allele in the polymorphic p53 enhancer leads to increased p53-dependent activation of the pro-survival target gene, *KITLG*, which increases TGCT survival rather than senescence/apoptosis in the presence of active p53. We demonstrate that co-inhibition of c-KIT and p53 activation interact synergistically to kill platinum-resistant TGCTs with a drug combination (Dasatinib and Doxorubicin) that had limited toxicity in a Phase II clinical trial (50), suggesting that an effective therapeutic strategy for treatment-resistant TGCTs could be to modulate both the cell-death and cell-survival functions of wtp53 cancers.

Using the most well-studied somatic mutation known to enhance KITLG/KIT signalling (cKIT mutations), we were able to identify SKCM as another potential repurposing opportunity for combination therapies which inhibit KITLG/KIT signalling and activate p53. The role of KIT signalling in the skin is well established with the pathway of crucial importance for the development of melanocytes (51). In line with previous work, we found wtp53 SKCM to be enriched for cKIT mutations (52,53). Furthermore, we found high KITLG expression to associate independently with poorer overall survival in wtp53 SKCM patients. Our data provides molecular support for targeting of KITLG/KIT in melanoma. Melanoma rarely mutates p53 and expresses high levels of wtp53 protein, in line with the fact that SKCM to be enriched for wtp53 and no p53 copy number loss (54). Melanomas are hardwired to be resistant to p53 dependent apoptosis, perhaps because melanocytes are programmed to survive UV light (55). Several mechanisms have been proposed for this inhibition of p53 triggered apoptosis, including the action of iASPP, deletion of the CDKN2A locus, aberrant phosphorylation of p53 and activation of MDM2 by downstream KIT signalling (55,56).

More recently, it has been shown that WNT5a signalling and wtp53 might co-operate in melanoma to drive cells into a slow cycling state which is therapy resistant (57). It is possible that KITLG/KIT-mediated inhibition of the p53-apoptotic response adds a further mechanism through which wtp53 can be inhibited in melanoma without mutation, and opens up the possibility of harnessing the pro-apoptotic function of p53 by inhibiting the KITLG/KIT pathway. Indeed, we showed that the combination of Dasatinib and Nutlin-3a and Dasatinib and Doxorubicin are synergistic in a wtp53 and KIT SKCM cell-line.

Unlike other tumor suppressors, complete loss of p53 activity is not a requirement for cancer initiation. Reduction of p53 activity below a critical threshold through mutations is apparently necessary and sufficient for cancer development (58). These mutations are primarily missense mutations that affect p53's ability to bind to DNA in a sequence-specific manner and regulate transcription of its target genes. These same mutations when found constitutionally result in Li-Fraumeni Syndrome: a syndrome comprising dramatic increase in cancer risk in many tissues types. These missense mutations may benefit cancers not simply through loss of p53 function, but also through dominant-negative and gain-of-function activities (59). In mice, knock-in p53 gain-of-function mutants displayed a more diverse set of, and more highly metastatic tumors than p53 knock-out mutants (60,61). Many of the factors that regulate wild-type p53 tumor suppression can also regulate mutant p53, including its pro-cancer activities. For example, wild-type p53 mice that express lower levels of MDM2 show increased p53 levels, a better p53 stress response, and greater tumor suppression, resulting in later and reduced tumor onset in many tissue types. Mutant p53 levels are also increased in these murine models, but cancers are found to arise earlier and harbor gain-of-function metastatic phenotypes (62).

We go on to discuss that our SNP association with inverted cancer risk and somatic p53 mutational status in humans reveal a similar scenario. Specifically, we demonstrated that the C-allele of the p53 poly(A) SNP which can lead to decreased wild type and mutant p53 levels in tumors, associates with an increased risk of wtp53 cancers, but decreased risk of sub-types with primarily mutant p53. For example, women with the minor allele associated with an increased risk for the more p53 wild-type breast and ovarian subtypes and a decreased risk for the more mutant subtypes. We also demonstrated that the TCGA pan-cancer or breast patients with wtp53 tumours and carrying the C allele have shorter PFI compared to patients with wtp53 tumours but without the C allele. Of note, an inverted trend was found for p53mut tumours. Together, these observations support a role for germline p53 pathway SNPs not only modulating risk of disease and tumor biology in wtp53

cancers but also in p53 mutant cancers, wherein alleles that increase mutant p53 levels would also increase its pro-cancer activities.

Acknowledgments

This work was funded in part by the Ludwig Institute for Cancer Research, the Nuffield Department of Medicine, the Development Fund, Oxford Cancer Research Centre, University of Oxford, UK, by the Intramural Research Program of the National Institute of Environmental Health Sciences-National Institutes of Health (Z01-ES100475), and NIH grant (DP5-OD017937), US, and by the S-CORT Consortium from the Medical Research Council and Cancer Research UK.

References

1. Dancey JE, Bedard PL, Onetto N, Hudson TJ. The genetic basis for cancer treatment decisions. Cell **2012**;148(3):409-20
2. Huang M, Shen A, Ding J, Geng M. Molecularly targeted cancer therapy: some lessons from the past decade. Trends Pharmacol Sci **2014**;35(1):41-50
3. Carter H, Marty R, Hofree M, Gross AM, Jensen J, Fisch KM, *et al.* Interaction Landscape of Inherited Polymorphisms with Somatic Events in Cancer. Cancer discovery **2017**;7(4):410-23
4. Lu C, Xie M, Wendl MC, Wang J, McLellan MD, Leiserson MD, *et al.* Patterns and functional implications of rare germline variants across 12 cancer types. Nature communications **2015**;6:10086
5. Yurgelun MB, Chenevix-Trench G, Lippman SM. Translating Germline Cancer Risk into Precision Prevention. Cell **2017**;168(4):566-70
6. Stracquadanio G, Wang XT, Wallace MD, Grawenda AM, Zhang P, Hewitt J, *et al.* The importance of p53 pathway genetics in inherited and somatic cancer genomes. Nature Reviews Cancer **2016**;16(4):251-65
7. Martincorena I, Raine KM, Gerstung M, Dawson KJ, Haase K, Van Loo P, *et al.* Universal Patterns of Selection in Cancer and Somatic Tissues. Cell **2017**;171(5):1029-41 e21
8. Kastenhuber ER, Lowe SW. Putting p53 in Context. Cell **2017**;170(6):1062-78
9. Bouwman P, Jonkers J. The effects of deregulated DNA damage signalling on cancer chemotherapy response and resistance. Nature reviews Cancer **2012**;12(9):587-98
10. Lowe SW, Ruley HE, Jacks T, Housman DE. P53-Dependent Apoptosis Modulates the Cytotoxicity of Anticancer Agents. Cell **1993**;74(6):957-67
11. Weinstein JN, Myers TG, O'Connor PM, Friend SH, Fornace AJ, Jr., Kohn KW, *et al.* An information-intensive approach to the molecular pharmacology of cancer. Science **1997**;275(5298):343-9
12. Willer CJ, Li Y, Abecasis GR. METAL: fast and efficient meta-analysis of genomewide association scans. Bioinformatics **2010**;26(17):2190-1
13. Liu JF, Lichtenberg T, Hoadley KA, Poisson LM, Lazar AJ, Cherniack AD, *et al.* An Integrated TCGA Pan-Cancer Clinical Data Resource to Drive High-Quality Survival Outcome Analytics. Cell **2018**;173(2):400-+
14. Ran FA, Hsu PD, Wright J, Agarwala V, Scott DA, Zhang F. Genome engineering using the CRISPR-Cas9 system. Nature protocols **2013**;8(11):2281-308

15. Zhang P, Elabd S, Hammer S, Solozobova V, Yan H, Bartel F, *et al.* TRIM25 has a dual function in the p53/Mdm2 circuit. Oncogene **2015**;34(46):5729-38
16. Chou TC. Theoretical basis, experimental design, and computerized simulation of synergism and antagonism in drug combination studies. Pharmacol Rev **2006**;58(3):621-81
17. Stacey SN, Sulem P, Jonasdottir A, Masson G, Gudmundsson J, Gudbjartsson DF, *et al.* A germline variant in the TP53 polyadenylation signal confers cancer susceptibility. Nature genetics **2011**;43(11):1098-103
18. Consortium GT. The Genotype-Tissue Expression (GTEx) project. Nature genetics **2013**;45(6):580-5
19. Deng Q, Hu H, Yu X, Liu S, Wang L, Chen W, *et al.* Tissue-specific microRNA expression alters cancer susceptibility conferred by a TP53 noncoding variant. Nature communications **2019**;10(1):5061
20. Rafnar T, Gunnarsson B, Stefansson OA, Sulem P, Ingason A, Frigge ML, *et al.* Variants associating with uterine leiomyoma highlight genetic background shared by various cancers and hormone-related traits. Nature communications **2018**;9(1):3636
21. Zhang H, Ahearn TU, Lecarpentier J, Barnes D, Beesley J, Qi G, *et al.* Genome-wide association study identifies 32 novel breast cancer susceptibility loci from overall and subtype-specific analyses. Nature genetics **2020**;52(6):572-81
22. Landi MT, Bishop DT, MacGregor S, Machiela MJ, Stratigos AJ, Ghiorzo P, *et al.* Genome-wide association meta-analyses combining multiple risk phenotypes provide insights into the genetic architecture of cutaneous melanoma susceptibility. Nature genetics **2020**;52(5):494-504
23. Rashkin SR, Graff RE, Kachuri L, Thai KK, Alexeeff SE, Blatchins MA, *et al.* Pan-cancer study detects genetic risk variants and shared genetic basis in two large cohorts. Nature communications **2020**;11(1):4423
24. Cancer Genome Atlas N. Comprehensive molecular portraits of human breast tumours. Nature **2012**;490(7418):61-70
25. Cancer Genome Atlas Research N. Integrated genomic analyses of ovarian carcinoma. Nature **2011**;474(7353):609-15
26. Michailidou K, Lindstrom S, Dennis J, Beesley J, Hui S, Kar S, *et al.* Association analysis identifies 65 new breast cancer risk loci. Nature **2017**;551(7678):92-4
27. Phelan CM, Kuchenbaecker KB, Tyrer JP, Kar SP, Lawrenson K, Winham SJ, *et al.* Identification of 12 new susceptibility loci for different histotypes of epithelial ovarian cancer. Nature genetics **2017**;49(5):680-91
28. Suh YA, Post SM, Elizondo-Fraire AC, Maccio DR, Jackson JG, El-Naggar AK, *et al.* Multiple stress signals activate mutant p53 in vivo. Cancer Res **2011**;71(23):7168-75
29. Yue X, Zhao Y, Xu Y, Zheng M, Feng Z, Hu W. Mutant p53 in Cancer: Accumulation, Gain-of-Function, and Therapy. J Mol Biol **2017**;429(11):1595-606
30. Burckstummer T, Banning C, Hainzl P, Schobesberger R, Kerzendorfer C, Pauler FM, *et al.* A reversible gene trap collection empowers haploid genetics in human cells. Nature methods **2013**;10(10):965-71
31. Gudkov AV, Komarova EA. The role of p53 in determining sensitivity to radiotherapy. Nature reviews Cancer **2003**;3(2):117-29
32. Hientz K, Mohr A, Bhakta-Guha D, Efferth T. The role of p53 in cancer drug resistance and targeted chemotherapy. Oncotarget **2017**;8(5):8921-46
33. Fischer M. Census and evaluation of p53 target genes. Oncogene **2017**;36(28):3943-56
34. Iorio F, Knijnenburg TA, Vis DJ, Bignell GR, Menden MP, Schubert M, *et al.* A Landscape of Pharmacogenomic Interactions in Cancer. Cell **2016**;166(3):740-54

35. Turnbull C, Rapley EA, Seal S, Pernet D, Renwick A, Hughes D, *et al.* Variants near DMRT1, TERT and ATF7IP are associated with testicular germ cell cancer. Nature genetics **2010**;42(7):604-U178
36. Litchfield K, Levy M, Orlando G, Loveday C, Law PJ, Migliorini G, *et al.* Identification of 19 new risk loci and potential regulatory mechanisms influencing susceptibility to testicular germ cell tumor. Nature genetics **2017**;49(7):1133-+
37. Zeron-Medina J, Wang X, Repapi E, Campbell MR, Su D, Castro-Giner F, *et al.* A polymorphic p53 response element in KIT ligand influences cancer risk and has undergone natural selection. Cell **2013**;155(2):410-22
38. Lennartsson J, Ronnstrand L. Stem cell factor receptor/c-Kit: from basic science to clinical implications. Physiological reviews **2012**;92(4):1619-49
39. Flaherty KT, Hodi FS, Fisher DE. From genes to drugs: targeted strategies for melanoma. Nature reviews Cancer **2012**;12(5):349-61
40. Dos Santos C, McDonald T, Ho YW, Liu H, Lin A, Forman SJ, *et al.* The Src and c-Kit kinase inhibitor dasatinib enhances p53-mediated targeting of human acute myeloid leukemia stem cells by chemotherapeutic agents. Blood **2013**;122(11):1900-13
41. Henze J, Muhlenberg T, Simon S, Grabellus F, Rubin B, Taeger G, *et al.* p53 Modulation as a Therapeutic Strategy in Gastrointestinal Stromal Tumors. Plos One **2012**;7(5)
42. Kurosu T, Wu N, Oshikawa G, Kagechika H, Miura O. Enhancement of imatinib-induced apoptosis of BCR/ABL-expressing cells by nutlin-3 through synergistic activation of the mitochondrial apoptotic pathway. Apoptosis : an international journal on programmed cell death **2010**;15(5):608-20
43. Litchfield K, Levy M, Huddart RA, Shipley J, Turnbull C. The genomic landscape of testicular germ cell tumours: from susceptibility to treatment. Nat Rev Urol **2016**;13(7):409-19
44. Noel EE, Yeste-Velasco M, Mao X, Perry J, Kudahetti SC, Li NF, *et al.* The association of CCND1 overexpression and cisplatin resistance in testicular germ cell tumors and other cancers. The American journal of pathology **2010**;176(6):2607-15
45. Koster R, di Pietro A, Timmer-Bosscha H, Gibcus JH, van den Berg A, Suurmeijer AJ, *et al.* Cytoplasmic p21 expression levels determine cisplatin resistance in human testicular cancer. The Journal of clinical investigation **2010**;120(10):3594-605
46. Buniello A, MacArthur JAL, Cerezo M, Harris LW, Hayhurst J, Malangone C, *et al.* The NHGRI-EBI GWAS Catalog of published genome-wide association studies, targeted arrays and summary statistics 2019. Nucleic acids research **2019**;47(D1):D1005-D12
47. Van Allen EM, Miao D, Schilling B, Shukla SA, Blank C, Zimmer L, *et al.* Genomic correlates of response to CTLA-4 blockade in metastatic melanoma. Science **2015**;350(6257):207-11
48. Vazquez A, Bond EE, Levine AJ, Bond GL. The genetics of the p53 pathway, apoptosis and cancer therapy. Nat Rev Drug Discov **2008**;7(12):979-87
49. Kruiswijk F, Labuschagne CF, Vousden KH. p53 in survival, death and metabolic health: a lifeguard with a licence to kill. Nat Rev Mol Cell Bio **2015**;16(7):393-405
50. Benjamini O, Dumlao TL, Kantarjian H, O'Brien S, Garcia-Manero G, Faderl S, *et al.* Phase II trial of HyperCVAD and Dasatinib in patients with relapsed Philadelphia chromosome positive acute lymphoblastic leukemia or blast phase chronic myeloid leukemia. American journal of hematology **2014**;89(3):282-7
51. Wehrle-Haller B. The role of Kit-ligand in melanocyte development and epidermal homeostasis. Pigment cell research / sponsored by the European Society for Pigment Cell Research and the International Pigment Cell Society **2003**;16(3):287-96
52. Beadling C, Jacobson-Dunlop E, Hodi FS, Le C, Warrick A, Patterson J, *et al.* KIT gene mutations and copy number in melanoma subtypes. Clin Cancer Res **2008**;14(21):6821-8

53. Curtin JA, Busam K, Pinkel D, Bastian BC. Somatic activation of KIT in distinct subtypes of melanoma. J Clin Oncol **2006**;24(26):4340-6
54. McGregor JM, Yu CC, Dublin EA, Barnes DM, Levison DA, MacDonald DM. p53 immunoreactivity in human malignant melanoma and dysplastic naevi. The British journal of dermatology **1993**;128(6):606-11
55. Box NF, Vukmer TO, Terzian T. Targeting p53 in melanoma. Pigment cell & melanoma research **2014**;27(1):8-10
56. Lu M, Breyssens H, Salter V, Zhong S, Hu Y, Baer C, *et al.* Restoring p53 function in human melanoma cells by inhibiting MDM2 and cyclin B1/CDK1-phosphorylated nuclear iASPP. Cancer cell **2013**;23(5):618-33
57. Webster MR, Fane ME, Alicea GM, Basu S, Kossenkov AV, Marino GE, *et al.* Paradoxical Role for Wild-Type p53 in Driving Therapy Resistance in Melanoma. Molecular cell **2020**;77(3):681
58. Hohenstein P. Tumour suppressor genes--one hit can be enough. PLoS biology **2004**;2(2):E40
59. Muller PA, Vousden KH. Mutant p53 in cancer: new functions and therapeutic opportunities. Cancer cell **2014**;25(3):304-17
60. Lang GA, Iwakuma T, Suh YA, Liu G, Rao VA, Parant JM, *et al.* Gain of function of a p53 hot spot mutation in a mouse model of Li-Fraumeni syndrome. Cell **2004**;119(6):861-72
61. Olive KP, Tuveson DA, Ruhe ZC, Yin B, Willis NA, Bronson RT, *et al.* Mutant p53 gain of function in two mouse models of Li-Fraumeni syndrome. Cell **2004**;119(6):847-60
62. Terzian T, Suh YA, Iwakuma T, Post SM, Neumann M, Lang GA, *et al.* The inherent instability of mutant p53 is alleviated by Mdm2 or p16INK4a loss. Genes & development **2008**;22(10):1337-44

Figure Legends

Figure 1. p53 regulatory cancer risk SNPs associate with subtype heterogeneity risk. (A) Pie charts of the percentages of oncogenic and loss-of-function p53 mutations found amongst all known pathogenic p53 missense mutations in breast and ovarian cancers. (B) A proposed model of how p53 poly(A) SNP could modify the ability of mutant p53 to drive cancer and of wild type p53 (wtp53) to suppress it. (C) Forest plots illustrating the associations of the p53 poly(A) SNP with breast cancer and ovarian cancer subtype heterogeneity. The odd ratios (OR) are plotted for the SNP and subtype, and the error bars represent the associated 95% confidence intervals (CI). (D) A schematic overview of the association testing between the SNP and p53 mutational status in TCGA tumors. (E) A bar plot of the minor allele frequencies (MAFs) of the p53 poly(A) SNP in patients with either wtp53 tumors or mutant p53 tumors.

Figure 2. A p53 regulatory cancer risk SNP and somatic copy number loss of p53 associates with clinical outcomes. (A) A box plot of p53 mRNA expression levels in 3,248 tumors from individuals with differing genotypes of the p53 poly(A) SNP. The fold change of median p53 expression between genotypes, the p-value (linear regression) and beta coefficients of the association of the genotype with mRNA levels are depicted. (B) A schematic diagram of the p53 mutational status and CRISPR-editing strategy in Hap1 cells. (C) A bar plot of p53 mRNA levels for each genotype in Hap1 cells, measured using qRT-PCR normalized to GAPDH. Error bars represent SEM of 3 independent experiments. p-values were calculated using a two-tailed t-test. (D) A forest plot of the PFI and OS of cancer patients (pan-cancer TCGA cohort) stratified by the somatic p53 mutational status. Hazard ratios (HR) and p values were calculated using Cox proportional hazards model.. (E) Kaplan-Meier survival curves for PFI in a total of 381 breast cancer patients carrying either the major or the minor allele of the p53 poly(A) SNP and/or somatic *TP53* mutations. Curves were truncated at 10 years, but the statistical analyses were performed using all of the data (logrank test). (F) A bar plot showing the percentage of non-responders in each group stratified by the somatic or germline p53 alterations as indicated on the x axis. Numbers of patients (number of non-responders / total number of patients) in each group are indicated within the bars. p values were calculated by two-tailed Fisher's exact test (*$p<0.05$, **$p<0.005$). (G) Box plots of p53 mRNA expression levels in p53wt tumors (left panel) and mutant p53 tumors (right panel) from individuals with differing p53 copy number status. (H) A forest plot of PFI and OS of TCGA cancer patients stratified by the somatic p53 mutational status. HR comparing PFI and OS in patients with or without p53 copy number loss are indicated on the right. (I) A bar plot showing the percentage of non-

responders in each group stratified by the p53 mutations and copy number loss as indicated on the x axis.

Figure 3. Copy number loss of p53 dampens p53's anti-cancer activities. (A) Box plots of p53 mRNA expression levels in p53wt cells (left panel) and mutant p53 cells (right panel) with differing p53 copy number status. (B) Volcano plots of 304 drugs and their association with differential sensitivity in cancer cell lines with p53 copy number loss relative to cell lines without p53 copy number loss (left: wtp53 cells; right: mutant p53 cells). -Log10 adjusted p-values (linear regression and FDR-adjusted) are plotted against the beta coefficient. The horizontal dashed lines represent the FDR-adjusted p value of 0.05. (C) A Chord Diagram of 102 cancer GWAS lead SNPs in 41 p53 pathway genes that associate differential risk to a total of 19 different cancer types. The width of the connecting band indicates the number of lead SNPs for each association. A dot plot of the odds ratios for each association is presented in the inner circle and with red dots. The median odd ratio for each association is presented in parentheses next to the gene name. (D) Volcano plots of the associations between the transcript levels of the 41 *TP53* pathway cancer GWAS genes and Nutlin3 sensitivities in cancer cell lines with either wtp53-no.loss (upper panel) or p53mutant-loss (lower panel). (E) Box plots of the Log2 IC50 values of p53 activating agents in cells either with low, intermediate or high KITLG mRNA levels and wtp53-no.loss.

Figure 4. The p53-bound cancer risk locus in *KITLG* associates with patient outcome and attenuates p53's anti-cancer activities. (A-B) Dot plots showing the enrichment of KITLG copy number gains (A) and risk allele frequencies (B) across TCGA cancer types. -Log10 adjusted p-values are plotted against the Log2 fold change of the percentage of tumors with KITLG gains/risk alleles in a given cancer type vs. the other cancers combined. (C) A Kaplan-Meier survival curve for PFI in p53wt testicular cancer patients with high or low KITLG mRNA expression. p value was calculated using log-rank test. (D) Genetic fine mapping identified 6 SNPs with the strongest TGCT GWAS signal and which are in high linkage disequilibrium (r2) in Europeans (red square). (E) A Kaplan-Meier survival curve for PFI in high-stage p53wt testicular cancer patients carrying either the risk (orange) or the non-risk allele (grey) of the KITLG risk SNP. (F) A diagram of the CRISPR-editing utilized. (G) KITLG gene expression in CRISPR-edited clones using qRT-PCR normalized to GAPDH. In total, 2 to 3 clones of each genotype were analyzed in 3 independent biological replicates. p-values were calculated using a one-way ANOVA, followed by Tukey's multiple comparison test. (H) A bar graph of the fold change in KITLG expression after Nutlin3 treatment,

Error bars represent SEM of 2 clones for each genotype and in 2 independent experiments. p-values were calculated using a two-tailed t-test. (I) Dot plots of KITLG expression in CRISPR-edited clones.

Figure 5. p53/*KITLG* pro-survival signaling can attenuate responses to p53-activating agents. (A) Bar blots of the IC50 values for Nutlin3. p-values were calculated using a two-tailed t-test and error bars represent SEM in at least 3 independent biological replicates. (B) Western blot analysis of cells that were treated with or without Nutlin3 for 6 hours, lysed and analyzed for p53, acetylated p53, Parp1 and cleaved-caspase3 protein expression. (C) Schematic overview for the microscopy-based high-content drug screening. (D) Bar plots depicting the number of hits and "non-hits" for each of the 14 drug classes examined. (E) Scatter plots of the fold enrichment of hits amongst each drug class relative to the total compounds in 14 drug classes. The horizontal dashed lines represent the FDR-adjusted p value of 0.05. (F-G) Bar plots of combination indexes of Dasatinib with Nutllin3 (F) or Doxorubincin (G) in p53-REs+/+ (grey bars, two clones), p53-REs-/- (red bars, two clones) and knock-in clones (orange bars, one clone) of TERA1 and TERA2 cells. (H) Bar plots of combination indexes of Dasatinib with Nutllin3 or Doxorubincin in panel of TGCT cell lines. (I) Growth curves of 2102EP xenograft tumors treated with vehicle, Doxorubicin, Dasatinib or the combination of Doxorubicin and Dasatinib. Error bars represent means ± SEM (n=6).

Figure 6. KITLG/c-KIT signaling interacts with p53 to affect cancer progression and drug response in melanoma. (A) A bar graph of the percentage of oncogenic c-KIT mutations in wtp53 tumors relative to p53 mutant tumors. (B) Scatter plots of the fold enrichment of oncogenic c-KIT mutations in a given cancer type relative to all cKIT mutation in pan-cancer. The horizontal dashed lines represent the FDR-adjusted p value of 0.05. (C-E) Kaplan-Meier survival curves for OS (C, left panel) and PFI (C, right panel) in TCGA-SKCM patients, for OS (D) in TCGA-AML patients, and for OS (E, left panel) and DFS (E, right panel) in DFCI-SKCM patients stratified based on KITLG mRNA levels. (F-G) Two forest plots of PFI and OS of TCGA cancer patients (F: SKCM; G: AML) stratified by the somatic p53 mutational status. HR and p values were calculated using Cox proportional hazards model. (H) A bar plot of combination indexes of Dasatinib with Nutllin3 or Doxorubincin in melanoma cells. p values were calculated by one-sample t-test. Error bars represent means ± SEM (n=3).

Figure 1

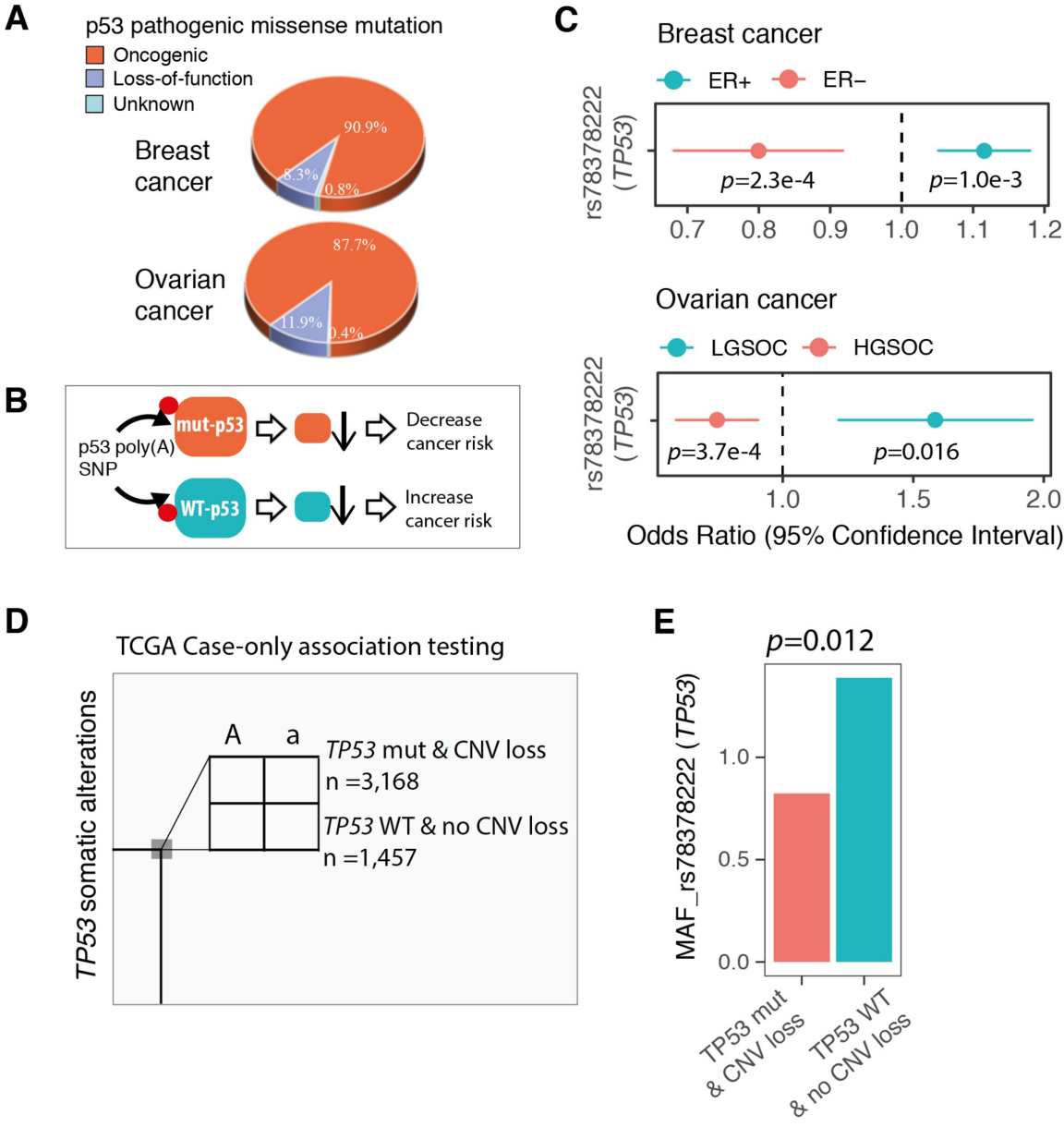
A
p53 pathogenic missense mutation
Oncogenic
Loss-of-function
Unknown
Breast cancer
90.9%
8.3%
0.8%
Ovarian cancer
87.7%
11.9%
0.4%
B
p53 poly(A) SNP
mut-p53
WT-p53
Decrease cancer risk
Increase cancer risk
C
Breast cancer
ER+
ER−
rs78378222 (TP53)
p=2.3e-4
p=1.0e-3
0.7
0.8
0.9
1.0
1.1
1.2
Ovarian cancer
LGSOC
HGSOC
rs78378222 (TP53)
p=3.7e-4
p=0.016
1.0
1.5
2.0
Odds Ratio (95% Confidence Interval)
D
TCGA Case-only association testing
TP53 somatic alterations
A
a
TP53 mut & CNV loss
n =3,168
TP53 WT & no CNV loss
n =1,457
E
p=0.012
MAF_rs78378222 (TP53)
1.0
0.5
0.0
TP53 mut & CNV loss
TP53 WT & no CNV loss

Figure 2

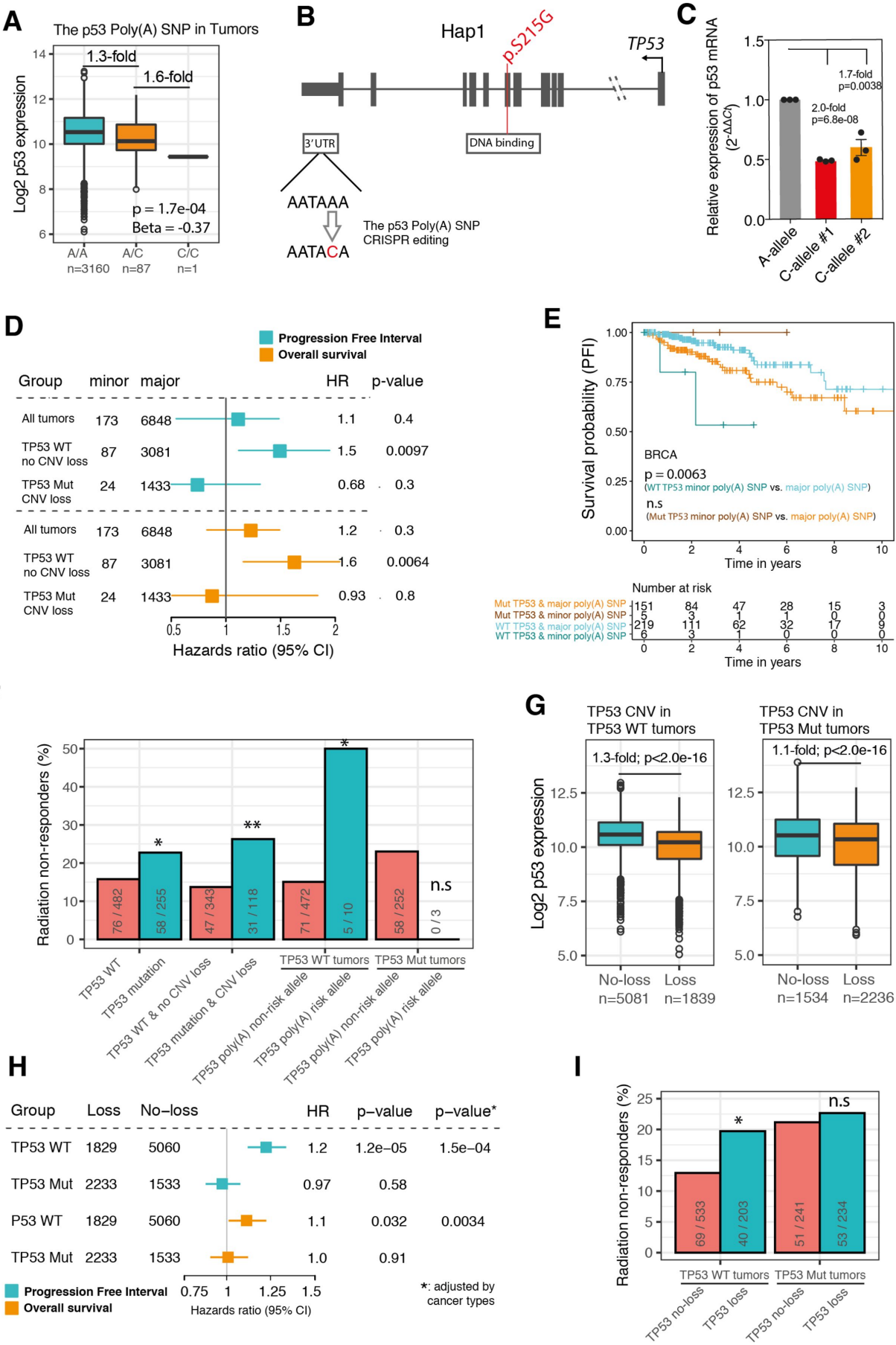
A
The p53 Poly(A) SNP in Tumors
1.3-fold
1.6-fold
Log2 p53 expression
p = 1.7e-04
Beta = -0.37
A/A n=3160
A/C n=87
C/C n=1
B
Hap1
p.S215G
TP53
3'UTR
DNA binding
AATAAA
AATACA
The p53 Poly(A) SNP CRISPR editing
C
Relative expression of p53 mRNA (2^-ΔΔCt)
1.7-fold p=0.0038
2.0-fold p=6.8e-08
A-allele
C-allele #1
C-allele #2
D
Progression Free Interval
Overall survival
Group minor major HR p-value
All tumors 173 6848 1.1 0.4
TP53 WT no CNV loss 87 3081 1.5 0.0097
TP53 Mut CNV loss 24 1433 0.68 0.3
All tumors 173 6848 1.2 0.3
TP53 WT no CNV loss 87 3081 1.6 0.0064
TP53 Mut CNV loss 24 1433 0.93 0.8
Hazards ratio (95% CI)
E
Survival probability (PFI)
BRCA
p = 0.0063
(WT TP53 minor poly(A) SNP vs. major poly(A) SNP)
n.s
(Mut TP53 minor poly(A) SNP vs. major poly(A) SNP)
Time in years
Number at risk
Mut TP53 & major poly(A) SNP 151 84 47 28 15 3
Mut TP53 & minor poly(A) SNP 5 3 1 0 0 0
WT TP53 & major poly(A) SNP 219 111 62 32 17 9
WT TP53 & minor poly(A) SNP 6 3 1 0 0 0
Time in years
F
Radiation non-responders (%)
76 / 482
58 / 255
47 / 343
31 / 118
71 / 472
5 / 10
58 / 252
0 / 3
n.s
TP53 WT
TP53 mutation
TP53 WT & no CNV loss
TP53 mutation & CNV loss
TP53 WT tumors
TP53 Mut tumors
TP53 poly(A) non-risk allele
TP53 poly(A) risk allele
TP53 poly(A) non-risk allele
TP53 poly(A) risk allele
G
TP53 CNV in TP53 WT tumors
1.3-fold; p<2.0e-16
TP53 CNV in TP53 Mut tumors
1.1-fold; p<2.0e-16
Log2 p53 expression
No-loss n=5081
Loss n=1839
No-loss n=1534
Loss n=2236
H
Group Loss No-loss HR p-value p-value*
TP53 WT 1829 5060 1.2 1.2e-05 1.5e-04
TP53 Mut 2233 1533 0.97 0.58
P53 WT 1829 5060 1.1 0.032 0.0034
TP53 Mut 2233 1533 1.0 0.91
Progression Free Interval
Overall survival
Hazards ratio (95% CI)
*: adjusted by cancer types
I
Radiation non-responders (%)
69 / 533
40 / 203
51 / 241
53 / 234
n.s
TP53 WT tumors
TP53 Mut tumors
TP53 no-loss
TP53 loss
TP53 no-loss
TP53 loss

Figure 3

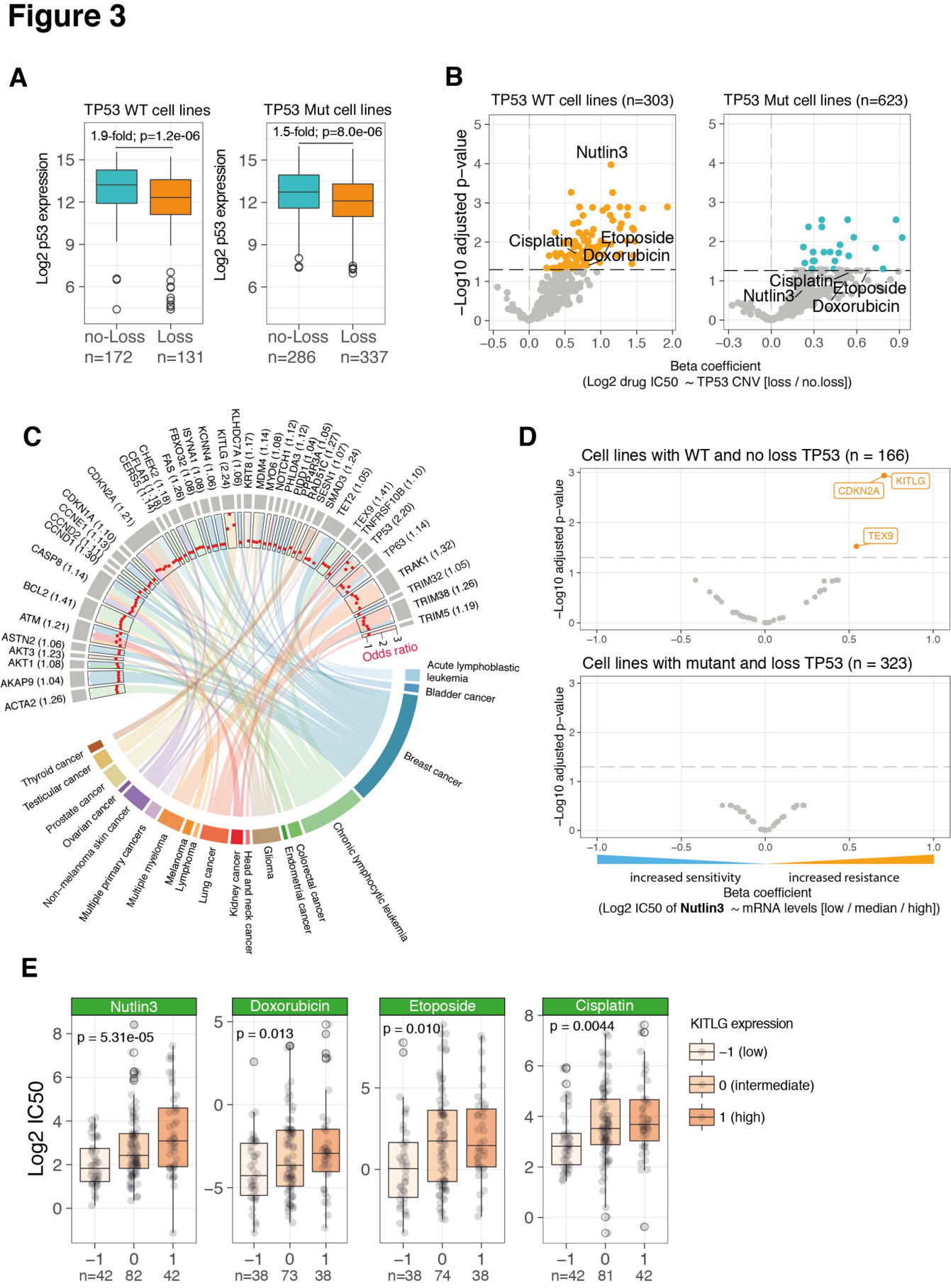
A
TP53 WT cell lines
1.9-fold; p=1.2e-06
Log2 p53 expression
no-Loss n=172
Loss n=131
TP53 Mut cell lines
1.5-fold; p=8.0e-06
no-Loss n=286
Loss n=337
B
TP53 WT cell lines (n=303)
TP53 Mut cell lines (n=623)
−Log10 adjusted p−value
Nutlin3
Cisplatin
Etoposide
Doxorubicin
Beta coefficient
(Log2 drug IC50 ~ TP53 CNV [loss / no.loss])
C
Odds ratio
Acute lymphoblastic leukemia
Bladder cancer
Breast cancer
Chronic lymphocytic leukemia
Colorectal cancer
Endometrial cancer
Glioma
Head and neck cancer
Kidney cancer
Lung cancer
Lymphoma
Melanoma
Multiple myeloma
Multiple primary cancers
Non−melanoma skin cancer
Ovarian cancer
Prostate cancer
Testicular cancer
Thyroid cancer
D
Cell lines with WT and no loss TP53 (n = 166)
Cell lines with mutant and loss TP53 (n = 323)
−Log10 adjusted p−value
CDKN2A
KITLG
TEX9
increased sensitivity
increased resistance
Beta coefficient
(Log2 IC50 of Nutlin3 ~ mRNA levels [low / median / high])
E
Nutlin3
Doxorubicin
Etoposide
Cisplatin
p = 5.31e-05
p = 0.013
p = 0.010
p = 0.0044
Log2 IC50
KITLG expression
−1 (low)
0 (intermediate)
1 (high)

Figure 4

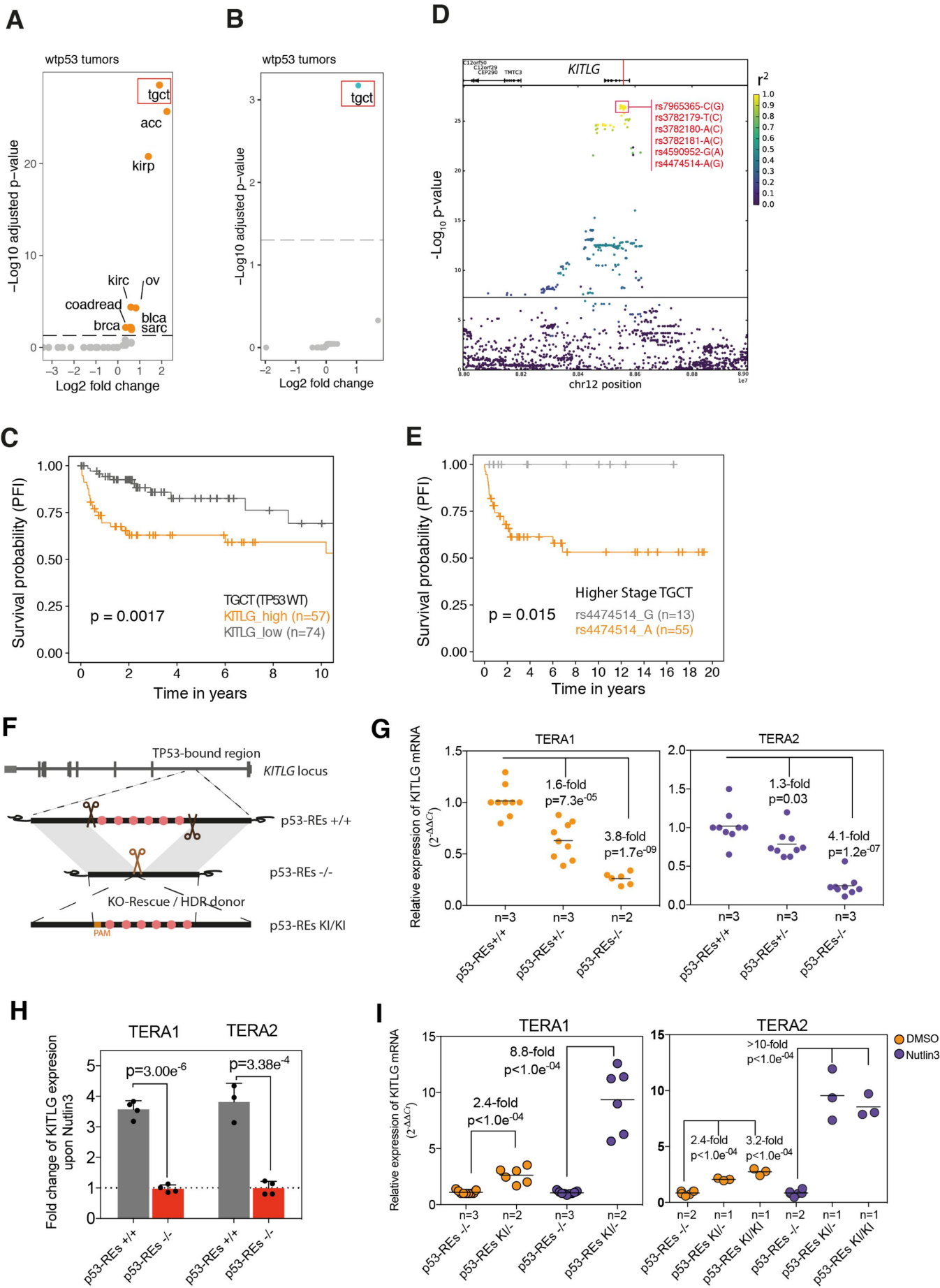
A
wtp53 tumors
−Log10 adjusted p−value
Log2 fold change
tgct
acc
kirp
kirc
ov
coadread
blca
brca
sarc
B
wtp53 tumors
−Log10 adjusted p−value
Log2 fold change
tgct
D
KITLG
r²
rs7965365-C(G)
rs3782179-T(C)
rs3782180-A(C)
rs3782181-A(C)
rs4590952-G(A)
rs4474514-A(G)
-Log10 p-value
chr12 position
C
Survival probability (PFI)
p = 0.0017
TGCT (TP53 WT)
KITLG_high (n=57)
KITLG_low (n=74)
Time in years
E
Survival probability (PFI)
p = 0.015
Higher Stage TGCT
rs4474514_G (n=13)
rs4474514_A (n=55)
Time in years
F
TP53-bound region
KITLG locus
p53-REs +/+
p53-REs -/-
KO-Rescue / HDR donor
p53-REs KI/KI
PAM
G
TERA1
TERA2
Relative expression of KITLG mRNA
1.6-fold
p=7.3e-05
3.8-fold
p=1.7e-09
1.3-fold
p=0.03
4.1-fold
p=1.2e-07
n=3
n=3
n=2
n=3
n=3
n=3
p53-REs+/+
p53-REs+/-
p53-REs-/-
H
TERA1
TERA2
Fold change of KITLG expression upon Nutlin3
p=3.00e-6
p=3.38e-4
p53-REs +/+
p53-REs -/-
I
TERA1
TERA2
Relative expression of KITLG mRNA
DMSO
Nutlin3
2.4-fold
p<1.0e-04
8.8-fold
p<1.0e-04
>10-fold
p<1.0e-04
3.2-fold
p<1.0e-04
p53-REs -/-
p53-REs KI/-
p53-REs KI/KI

Figure 5

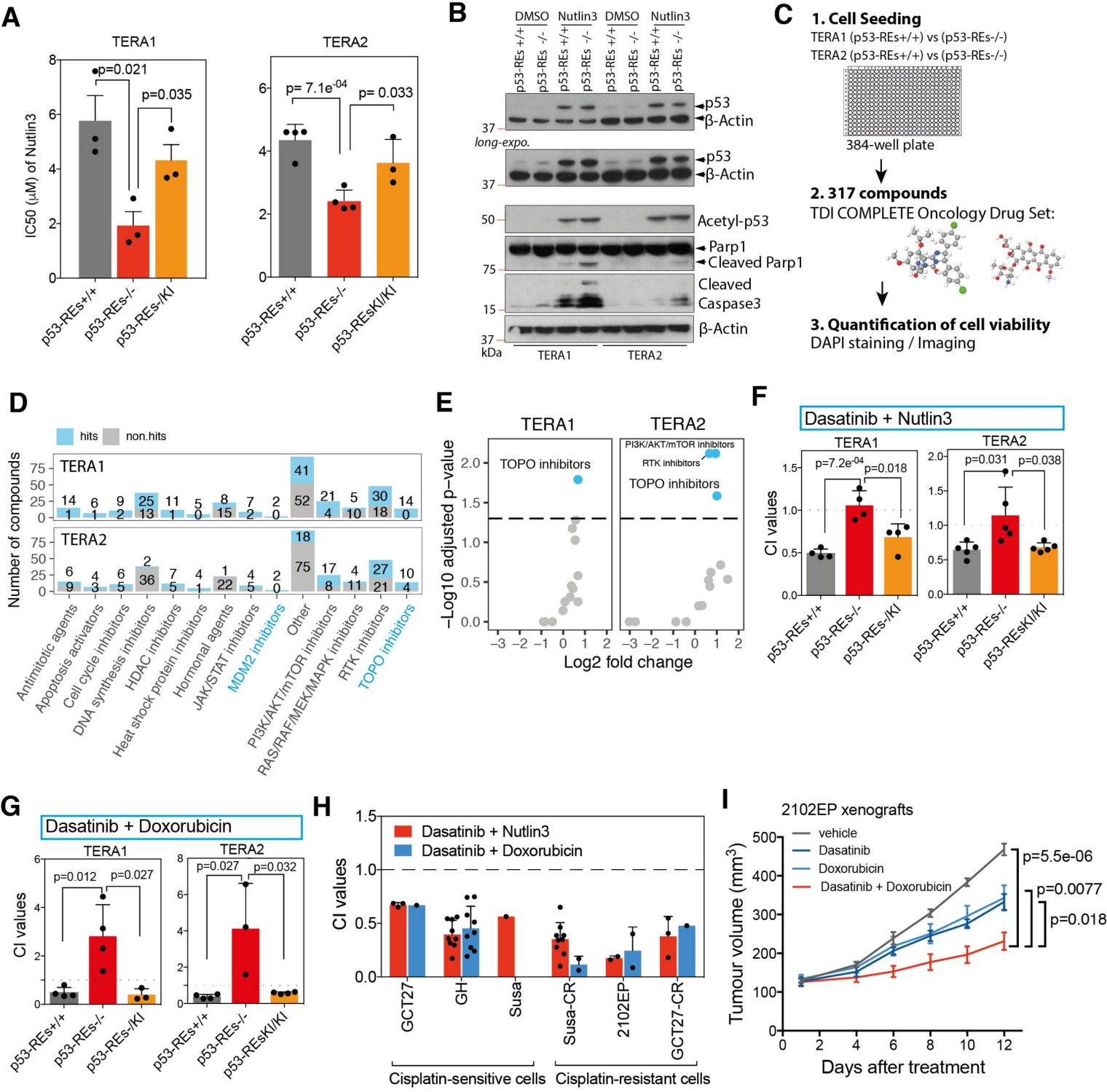
A
TERA1
TERA2
IC50 (μM) of Nutlin3
p=0.021
p=0.035
p= 7.1e-04
p= 0.033
p53-REs+/+
p53-REs-/-
p53-REs-/KI
p53-REsKI/KI
B
DMSO
Nutlin3
DMSO
Nutlin3
p53-REs +/+
p53-REs -/-
p53-REs +/+
p53-REs -/-
p53-REs +/+
p53-REs -/-
p53-REs +/+
p53-REs -/-
p53
β-Actin
long-expo.
p53
β-Actin
Acetyl-p53
Parp1
Cleaved Parp1
Cleaved Caspase3
β-Actin
kDa
TERA1
TERA2
C
1. Cell Seeding
TERA1 (p53-REs+/+) vs (p53-REs-/-)
TERA2 (p53-REs+/+) vs (p53-REs-/-)
384-well plate
2. 317 compounds
TDI COMPLETE Oncology Drug Set:
3. Quantification of cell viability
DAPI staining / Imaging
D
hits
non.hits
TERA1
TERA2
Number of compounds
Antimitotic agents
Apoptosis activators
Cell cycle inhibitors
DNA synthesis inhibitors
HDAC inhibitors
Heat shock protein inhibitors
Hormonal agents
JAK/STAT inhibitors
MDM2 inhibitors
Other
PI3K/AKT/mTOR inhibitors
RAS/RAF/MEK/MAPK inhibitors
RTK inhibitors
TOPO inhibitors
E
TERA1
TERA2
PI3K/AKT/mTOR inhibitors
RTK inhibitors
TOPO inhibitors
TOPO inhibitors
–Log10 adjusted p-value
Log2 fold change
F
Dasatinib + Nutlin3
TERA1
TERA2
CI values
p=7.2e-04
p=0.018
p=0.031
p=0.038
p53-REs+/+
p53-REs-/-
p53-REs-/KI
p53-REsKI/KI
G
Dasatinib + Doxorubicin
TERA1
TERA2
CI values
p=0.012
p=0.027
p=0.027
p=0.032
p53-REs+/+
p53-REs-/-
p53-REs-/KI
p53-REsKI/KI
H
Dasatinib + Nutlin3
Dasatinib + Doxorubicin
CI values
GCT27
GH
Susa
Susa-CR
2102EP
GCT27-CR
Cisplatin-sensitive cells
Cisplatin-resistant cells
I
2102EP xenografts
vehicle
Dasatinib
Doxorubicin
Dasatinib + Doxorubicin
Tumour volume (mm3)
Days after treatment
p=5.5e-06
p=0.0077
p=0.018

Figure 6

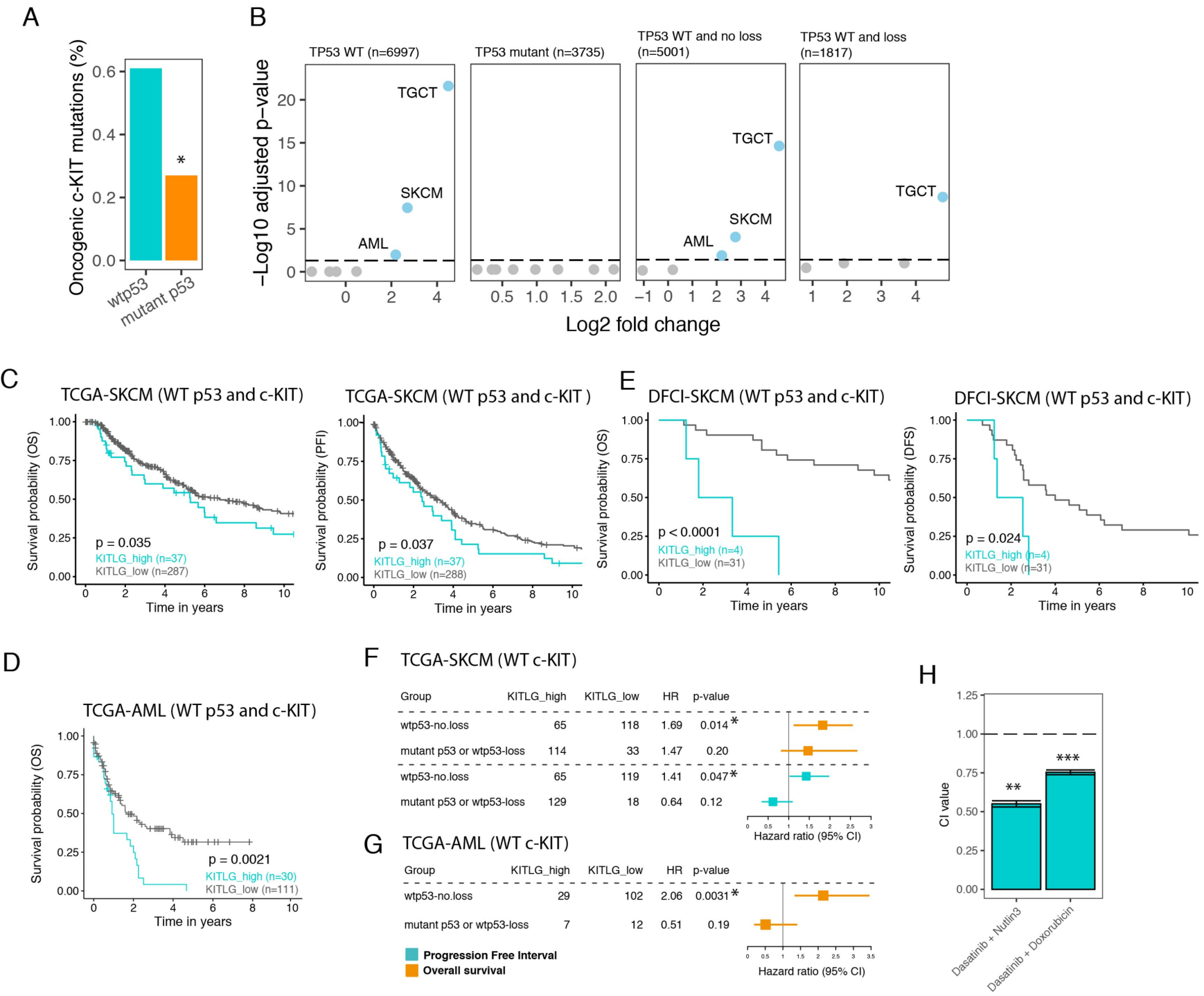
A
Oncogenic c-KIT mutations (%)
0.6
0.4
0.2
0.0
*
wtp53
mutant p53
B
TP53 WT (n=6997)
TP53 mutant (n=3735)
TP53 WT and no loss (n=5001)
TP53 WT and loss (n=1817)
−Log10 adjusted p−value
TGCT
SKCM
AML
Log2 fold change
C
TCGA-SKCM (WT p53 and c-KIT)
Survival probability (OS)
p = 0.035
KITLG_high (n=37)
KITLG_low (n=287)
Time in years
TCGA-SKCM (WT p53 and c-KIT)
Survival probability (PFI)
p = 0.037
KITLG_high (n=37)
KITLG_low (n=288)
Time in years
E
DFCI-SKCM (WT p53 and c-KIT)
Survival probability (OS)
p < 0.0001
KITLG_high (n=4)
KITLG_low (n=31)
Time in years
DFCI-SKCM (WT p53 and c-KIT)
Survival probability (DFS)
p = 0.024
KITLG_high (n=4)
KITLG_low (n=31)
Time in years
D
TCGA-AML (WT p53 and c-KIT)
Survival probability (OS)
p = 0.0021
KITLG_high (n=30)
KITLG_low (n=111)
Time in years
F
TCGA-SKCM (WT c-KIT)
Group KITLG_high KITLG_low HR p-value
wtp53-no.loss 65 118 1.69 0.014*
mutant p53 or wtp53-loss 114 33 1.47 0.20
wtp53-no.loss 65 119 1.41 0.047*
mutant p53 or wtp53-loss 129 18 0.64 0.12
Hazard ratio (95% CI)
G
TCGA-AML (WT c-KIT)
Group KITLG_high KITLG_low HR p-value
wtp53-no.loss 29 102 2.06 0.0031*
mutant p53 or wtp53-loss 7 12 0.51 0.19
Progression Free Interval
Overall survival
Hazard ratio (95% CI)
H
CI value
**
***
Dasatinib + Nutlin3
Dasatinib + Doxorubicin